Heliyon 9 (2023) e22016

Contents lists available at ScienceDirect

Heliyon

journal homepage: www.cell.com/heliyon

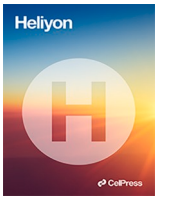

Pharmacokinetic and pharmacodynamic drug-drug interaction of Nomilin with atorvastatin in hyperlipidemic mice

Yan Ding [a,1], Huida Guan [b,1], Yingxuan Yan [a], Yan Chen [b], Cheng Huang [a,*]

[a] School of Pharmacy, Shanghai University of Traditional Chinese Medicine, 1200 Cailun Road, Shanghai, 201203, China
[b] Institute of Chinese Materia Medica, Shanghai University of Traditional Chinese Medicine, 1200 Cailun Road, Shanghai, 201203, China

ARTICLE INFO

Keywords:
Atorvastatin
Cytochrome P450
Drug-drug interaction
Nomilin
Pharmacodynamics
Pharmacokinetics

ABSTRACT

Atorvastatin (Atv) is widely used to lower cholesterol levels and treat hyperlipidemia in clinical application. Nomilin (Nom) is a kind of limonoids, which is found and isolated from the citrus herbs of *Rutaceae* family, which are widely used as patent medicines, functional foods, and nutritional supplements in many countries. In previous studies, Nom has the effect of anti-obesity and curing other metabolic diseases. Nevertheless, in recent years, the drug-drug interaction (DDI) caused by the administration of drugs with synergistic effects have raised worldwide concerns. To investigate the DDI of Nom and Atv *in vivo*, the pharmacokinetic studies were performed with using C57BL/6 mice. The plasma concentrations of Nom and Atv were measured after oral administration of different drug combinations by a simple and sensitive UHPLC-MS/MS method. The experimental mice were randomly divided into five groups, including control group, model group, administered Nom individually group, administered Atv individually group and co-administered of Nom and Atv group. The lipid levels including total cholesterol (TC), triglycerides (TG), high density lipoproteins-cholesterol (HDL-C), low density lipoproteins-cholesterol (LDL-C) were measured for pharmacodynamic study. The hepatic microsomal Cytochrome P450 (CYP1A2, CYP2E1 and CYP3A11) activities were probed using cocktail assay. The gene and protein expressions of CYP3A11 were detected via qPCR and Western blot method. The results shown that the area under the plasma concentration-time curve (AUC) of Atv in administered Atv individually group was 69.30 ± 15.45 ng/mL × h, while that of combined Nom with Atv group was 42.37 ± 10.15 ng/mL × h ($p < 0.05$). The degree of reduction in lipid levels of mice treated with co-administration of Atv and Nom was less than that of mice treated with Atv alone. In addition, Nom could cause an increased hepatic microsomal CYP3A11 activity significantly, and induce the gene levels and protein expressions of CYP3A11 elevated in mice livers. In conclusion, Nom could up-regulate CYP3A11 activity, thereby impacting on the pharmacokinetic profile and pharmacodynamic effect of Atv. The findings provide more insight for the use risk of these two drugs to treat hyperlipidemia diseases.

1. Introduction

Hyperlipidemia, a common metabolic disorder, is caused by abnormal fat metabolism function. Hyperlipidemia include

* Corresponding author.
E-mail address: chuang@shutcm.edu.cn (C. Huang).
[1] Yan Ding and Huida Guan contributed equally to this work.

https://doi.org/10.1016/j.heliyon.2023.e22016
Received 9 October 2023; Accepted 2 November 2023
Available online 7 November 2023

hypertriglyceridemia as well as mixed hyperlipidemia, in which both total cholesterol (TC), triglycerides (TG) levels are elevated. In addition, it involves an imbalance of cholesterol levels, including low-density lipoprotein cholesterol (LDL-C) and high-density lipoprotein cholesterol (HDL-C) in the blood. The LDL-C and HDL-C regulate the amount of cholesterol in the body and an imbalance can increase the risk of cardiovascular events, including myocardial infarction and stroke [1,2].

Statins, hydroxymethyl glutaryl-CoA (HMG-CoA) reductase inhibitors [3], are known as the most safe and effective choices for lowering cholesterol levels, among which atorvastatin (Atv) is widely used [4–6]. Atv has approximately 12 % oral bioavailability by the reason of substantial first-pass effect [7], when administered orally due to pre-systemic clearance (CL) in intestine and metabolism in the liver involving cytochrome P450 (CYP450) 3A4 enzyme (mouse CYP3A11 is a homolog to human CYP3A4) [8]. The CYP450 enzymes are involved in about 80 % of drug oxidative metabolism and approximately 50 % of the common medicine [9]. As the substrate of CYP3A4 isozyme, when Atv being co-administered with other medications, shows susceptibility to inhibitors and inducers of CYP3A4, which lead to increased or decreased plasma concentrations [10]. For instance, it was reported that when Atv was co-administered with CYP3A4 inhibitor itraconazole, the plasma exposure of Atv would significantly increase [11].

Limonoids are an important triterpenoids found in the *Rutaceae* family, which are widely used as patent medicines, functional foods and nutritional supplements in many countries [12]. Nomilin (Nom) is a kind of limonoids, which is found mostly in common edible citrus fruits, including lemons, oranges, grapefruits, mandarins, along with traditional Chinese medicines derived from citrus fruits, such as tangerine seed and tangerine peel [13]. Citrus herbs are often used in traditional medicine and can be taken concomitantly with conventional medicine [14]. In addition, as a main ingredient of the citrus herbs, Nom has a wide range of potential therapeutic effects such as anti-inflammatory [15], anticancer [16], antioxidant [17], anti-hyperglycemic activity and anti-obesity properties [18].

Hence, the concomitant use of statins drugs with Nom for lowering lipids may lead to potential drug-drug interaction (DDI). Currently numerous researches are mostly focused on the evaluation of DDI of drugs content *in vivo* of commonly herbal extracts and conventional drugs, and lacking pharmacodynamic evaluation [19,20]. Therefore, understanding the potential therapeutic role of botanicals and promote their safe and appropriate use, evaluation of efficacy, and exploring mechanism of action, are particularly important and urgent.

To our knowledge, there is no bioanalytical method reported for simultaneous quantification of Atv and Nom in any biological matrix until now, and the possible DDI mechanism was still not elucidated. In the present study, a simple, accurate and sensitive UHPLC-MS/MS method was developed to study the pharmacokinetic effect and the most crucial indexes of blood lipids were detected to investigate pharmacodynamic effect of Atv after the co-administration with Nom by oral route in healthy and hyperlipemia mice. The possible DDI mechanism was explored via metabolic enzyme pathway.

2. Materials and methods

2.1. Materials and reagents

Nomilin (Nom), atorvastatin (Atv) and rosuvastatin (IS) were got from Yuanye Bio-Technology Co., Ltd (Shanghai, China), and the structures of them were shown in Fig. 1. Phenacetin, acetaminophen, chlorzoxazone, 6-OH-chlorzoxazone, testosterone, 6β–OH–testosterone and NADPH regeneration system were purchased from Sigma-Aldrich (St. Louis, MO, USA). Carboxymethylcellulose sodium was obtained from Meilunbio Co. Ltd (Dalian, China). The RNAfast200 kit was purchased from Fastagen Biology, Co., Ltd. (Shanghai, China). The EvoM-MLV reverse transcription kit and SYBR® Green Pro Taq HS Master Mix was obtained from Accurate Biology, Co., Ltd. (Hunan, China). The BCA protein quantification kit was acquired from YEASEN Biotechnology, Co., Ltd. (Shanghai, China). The CYP3A11 and GAPDH antibodies were acquired from Protein Tech (Rosemont, USA). HPLC-grade methanol and acetonitrile were obtained from Fisher Scientific (New Jersey, USA). Ultra-pure water was filtered using the Milli-Q system (Millipore, Bedford, USA). All other chemicals used in this experiment were analytical grade.

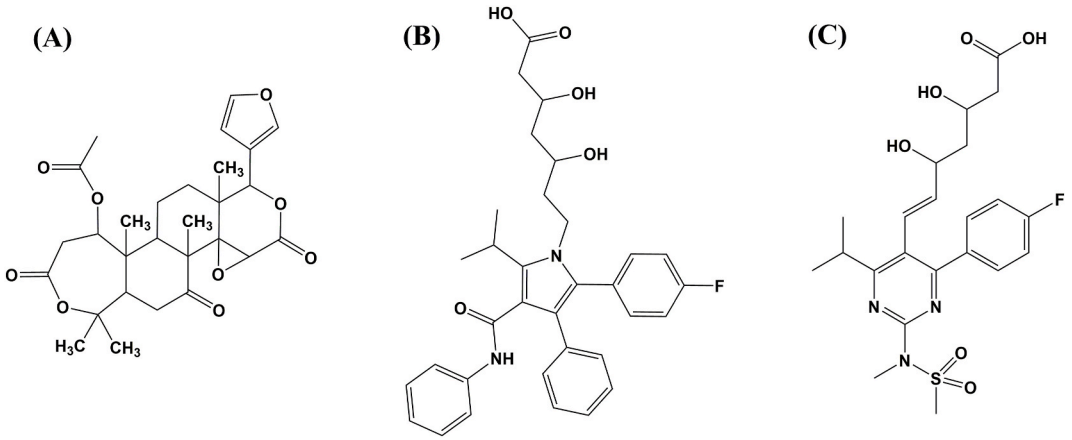

Fig. 1. The structures of Nomilin (A), Atorvastatin (B) and Rosuvastatin (C).

2.2. Ethics and animals

Male C57BL/6 mice (22–25 g) were supplied by Shanghai Sippe-Bk Lab Animal Co., Ltd. (Shanghai, China). Animals were housed in the Experimental Animal Center of Shanghai University of Traditional Chinese Medicine. Mice were acclimatized for 7 days before the start of experiments. Animals were kept in a controlled environment with consistent temperature and humidity, 12-h light/12-h dark cycle, as well as abundant food and water. The animal experimental research was approved by the Animal Care and Use Committee of Shanghai University of Traditional Chinese Medicine (Approval Number: PZSHUTCM220628001).

2.3. Establishment of hyperlipidemic model and group administration

Experimental animals were randomly divided into five groups of eight animals each. Hyperlipidemia was induced high fat diet (Common feed 78.8 %, cholesterol 1 %, cow bile salt 0.2 %, egg yolk powder 10 %, lard 10 %, Research Diets Co. Ltd, New Brunswick, USA) for three months except control group. The five grams of carboxymethylcellulose sodium powder were fully swollen in 1 L aqueous solution as 0.5 % CMC solution. The animals were then intragastric administration of drug solution once a day for 14 days. The specific groups were as follows, Group I: animals of normal diet administered with 0.5 % CMC solution served as control group; Group II: animals of high fat diet administered with same volume of 0.5 % CMC solution as model group; Group III: animals of high fat diet administered with 0.5 % CMC solution contained Nom (50 mg/kg); Group IV: animals of high fat diet administered with 0.5 % CMC solution contained Atv (1.67 mg/kg); Group V: animals of high fat diet co-administered with 0.5 % CMC solution contained Nom (50 mg/kg) and Atv (1.67 mg/kg).

2.4. Analysis conditions

For the pharmacokinetic study, a UHPLC-MS/MS system, performed on a 6500 QTRAP system (AB Sciex, CA, USA) equipped with ESI mode and coupled to a Shimadzu 30 A UHPLC system (Shimadzu, Kyoto, Japan) was used for the analysis of biological samples. The ESI source was set in positive ionization mode with the capillary voltage set at 5500 V. The dwell time was 100 ms, and the other parameters in the source were set as the following: source temperature was 550 °C; the nitrogen was used as the nebulizer and auxiliary gas, and the flow rates of nebulizer gas (Gas 1), heater gas (Gas 2), and curtain gas were set to 55, 55, and 35 L/min, respectively. The mass spectrometer scanned in multiple reactions monitoring (MRM) mode. The mass spectrometer was operated in positive ion mode using MRM to assess Nomilin (Nom), Atorvastatin (Atv) and Rosuvastatin (IS): m/z 515.5 → 161.1 for Nom; m/z 559.5 → 440.4 for Atv; m/z 482.5 → 258.2 for IS. The optimized declustering potential (DP) and collision energy (CE) were 160 eV and 32 V for Nom; 80 eV and 28 V for Atv; 80 eV and 42 V for IS respectively. The separation of all samples was obtained with an ACQUITY UPLC ®BEH C_{18} (2.1 × 50 mm, 1.7 μm) reversed-phase column. The autosampler was set at 10 °C, and the gradient elution was employed with 0.1 % formic acid aqueous solution as solvent A and 0.1 % formic acid acetonitrile solution as solvent B. The gradient program was as follows: 0–0.5 min, 35 % B; 0.5–1.5 min, 35–70 % B; 1.5–2.5 min, 70 % B; 2.5–2.6 min, 70–35 % B; 2.6–4 min, 35 % B. The flow rate was set at 0.4 mL/min, the column temperature was set to 45 °C and the injection volume was 5 μL. The total run time was 4 min for each sample.

2.5. Sample preparation

The liquid-liquid extraction method (LLE) with ethylacetate was finally chosen to prepare samples with comprehensive consideration and previous research [21]. Total of 100 μL ethylacetate containing IS solution (50 ng/mL) was added to 20 μL plasma sample in a clean centrifuge tube. The mixture was vortexed for 1 min and then centrifuged at 13,000 rpm for 10 min. After centrifugation, the organic layer was then separated and evaporated to dryness in a nitrogen blowing instrument (AutoVap S60E, ATR, USA) set at 40 °C. The residuals were reconstituted with 100 μL of initial mobile phase and then 5 μL supernatant was injected into the LC-MS/MS system for analysis.

2.6. Method validation

The method validation was validated according to the United States Food and Drug Administration (FDA) bioanalytical method validation guidelines [22]. The items of validation included selectivity, linearity, precision, accuracy, matrix effect, extraction recovery, and stability. The complete procedure for method validation was contained in the Supplementary materials Section 1.1-1.5.

2.7. Sample collection for pharmacokinetic study

Approximately 50 μL of blood was collected from individual mouse of five groups from retro-orbital plexus in eppendorf tubes at the time 15, 30, 60, 120, 240, 480 and 720 min after the last administration. Then the blood samples were centrifuged at 4500 rpm for 15 min immediately. The supernatants were separated and stored at −20 °C until analysis.

2.8. Estimation of the serum lipid levels for pharmacodynamic study

The residual blood was collected after the last blood collection point. The blood samples were also centrifuged at 4 °C at 4500 rpm for 15 min, and the supernatants were separated and then stored at −80 °C for estimation of lipid levels. The lipid levels of total

cholesterol (TC), triglycerides (TG), high density lipoproteins-cholesterol (HDL-C), low density lipoproteins-cholesterol (LDL-C) were measured by automatic biochemical instrument (HITACHI, Japan).

2.9. Histopathology assessment

The livers were collected from all mice sacrificed after collecting blood. The liver of every mouse was divided into three parts: one part was stored in 4 % paraformaldehyde for 7 days and sliced into coronal sections of 5–8 μm thickness for hematoxylin and eosin (HE) staining; one part was used to prepared as hepatic microsomes; while the other part was used for western blotting and quantitative real-time polymerase chain reaction experiments.

2.10. Determination of hepatic microsomal CYP450 enzyme activities

The hepatic microsomes were prepared by sequential ultracentrifugation, first at 9000 g for 10 min and then at 100,000 g for 1 h [23]. The concentrations of mice hepatic microsomes were calibrated using the protein concentration of each sample by BCA protein quantification kit (Yeasen Co. Ltd, Shanghai.). Three different enzyme substrates, phenacetin for CYP1A2, chlorzoxazone for CYP2E1 and testosterone for CYP3A4 (mouse CYP3A11 is a homolog to human CYP3A4), were used as probes to incubate with hepatic microsomes, and verapamil was the internal standard. The microsomal incubation mixture (a total volume of 250 μL) contained 1 mg/mL mouse liver microsomes, 0.1 M potassium phosphate buffer (PBS, pH 7.4), 10 mM $MgCl_2$, substrate cocktail. The NADPH regeneration system (1 mM $NADP^+$, 5 mM glucose 6-phosphate and 1 U/mL glucose 6-phosphate dehydrogenase) was added after pre-incubation of 5 min at 37 °C. Following the incubation reaction proceeded at 37 °C for 10 min (under a linear condition), and was terminated by adding 250 μL ice-cold acetonitrile (containing an internal standard) and centrifuged at 13,000 rpm under 4 °C for 15 min. The metabolites (acetaminophen, 6-OH-chlorzoxazone, 6β–OH–testosterone) of these CYPs probe substrates in all samples were determined using previously reported methods with slight modifications [24]. The analysis conditions were displayed in the Supplementary material Section 2.1.

2.11. Quantitative real-time polymerase chain reaction

The total RNA was extracted from mice liver tissues by using RNAfast200 kit according to the manufacturer's instructions. The content of total RNA of every sample was determined by measuring optical density at 260 nm. The cDNA was synthesized from total RNA by using an EvoM-MLV reverse transcription kit. Quantitative real-time polymerase chain reaction (qPCR) was performed on the Real-Time PCR system (Applied Biosystems, USA) using SYBR® Green Pro Taq HS Master Mix kit. The relative expression of CYP3A11 gene was normalized to GAPDH. The results were analyzed using the $2-\Delta\Delta Ct$ method and given as a ratio compared with the control group. The primer sequences were listed as follows: CYP3A11-F: CATCGCGGTAACCGTCCTC; CYP3A11-R: CCGCAGTTTTACTCCGAAG; GAPDH-F: GATGCTGGTGCTGAGTATGCG; GAPDH-R: GTGGTGCAGGATGCATTGCTCTGA.

2.12. Western blotting analysis

The total proteins were extracted from the mice liver tissues using RIPA lysis buffer and the protein quantifications were performed using a BCA protein assay kit. Every sample was normalized to the 20 μg of protein concentration. The protein extracts were separated in 10 % sodium dodecyl sulfate polyacrylamide gel electrophoresis (SDS-PAGE) and electrophoretically transferred onto polyvinylidene fluoride (PVDF) membranes. After being blocked with 5 % bovine serum albumin for 2 h at room temperature, the PVDF membranes were incubated at 4 °C overnight with primary antibodies, including CYP3A11 and GAPDH. The membranes were washed 3 times with TBST and incubated with secondary antibodies for 2 h at room temperature. The protein bands were visualized using enhanced chemiluminescence (ECL) reagent and quantified by calculating the gray densities of the target protein blots with internal controls.

2.13. Data analysis

Statistical analysis was performed using One-way ANOVA followed by Dunnett's multiple comparisons test of GraphPad Prism version 8.0 (GraphPad Software, CA, USA). The differences were considered to be significant statistically at $*p < 0.05$, $**p < 0.01$, $***p < 0.001$.

3. Results and discussion

3.1. Method optimization

3.1.1. Selectivity

In comparison with the MRM chromatograms of blank plasma samples (A), blank plasma samples spiked with Nom, Atv and IS (B), and plasma samples at 30 min after co-administered with Atv (1.67 mg/kg) and Nom (50 mg/kg) (C) (Fig. 2), no impurities that would interfere with the quantitation of analytes were observed, indicating that the established method has a good selectivity.

3.1.2. Linearity

The calibration curves were constructed by plotting the ratio of the peak areas of Nom or Atv to IS versus the concentration of Nom or Atv by using least-squares linear regression weighted by $1/x^2$. An excellent linearity was observed over the range of 1–500 ng/mL for Nom ($Y = 0.00373X\text{-}0.06925$, $R^2 = 0.9991$) and 0.1–100 ng/mL for Atv ($Y = 2952.18X{+}3.55 \times E^6$, $R^2 = 0.9997$).

3.1.3. Precision and accuracy

Precision and accuracy of the analytes in QC samples at four concentration levels were shown in Supplementary Material Table S1. For Nom, the intra-day precision (CV%) ranged from 3.57 % to 7.17 % and the inter-day precision (CV%) ranged from 3.02 % to 10.40 %. The intra-day and inter-day accuracies were ranged from −2.61 % to 6.82 % and −4.35 %–8.65 %. For Atv, the intra-day precision (CV%) ranged from 1.99 % to 4.28 % and the inter-day precision (CV%) ranged from 2.62 % to 9.61 %. The intra-day and inter-day accuracies were ranged from −6.36 % to 3.82 % and −6.88 %–8.15 %. The results were indicated that the established method was accurate, reproducible and reliable for quantitative analysis of the Nom and Atv in plasma samples.

3.1.4. Matrix effect and extraction recovery

At four concentrations for Nom, the matrix effect ranged from 90.23 ± 2.25 % to 94.07 ± 3.83 %, and the extraction recovery rate ranged from 76.61 ± 5.36 % to 79.21 ± 2.80 %. At four concentrations for Atv, the matrix effect ranged from 91.98 ± 5.46 % to 95.69 ± 8.87 %, and the extraction recovery rate ranged from 82.49 ± 5.11 % to 88.93 ± 5.85 %. Meanwhile, the matrix effect and extraction recovery of IS were 94.10 ± 2.66 % and 89.55 ± 2.85 %. As the results showed in Supplementary Material Table S1, the extraction method was stable and effective. No significant ion suppression or enhancement was observed in the analytical condition.

3.1.5. Stability

Short-term, long-term, freeze-thaw, and post-processed stabilities were determined using the QC samples at four concentrations, and the results were summarized in Supplementary Material Table S2. The absolute values of relative error (RE%) were all less than 15.00 %, indicating that the Nom and Atv were stable in rat plasma under predetermined storage conditions.

3.2. Pharmacokinetic analysis

The validated UHPLC-MS/MS method was successfully applied to the comparative pharmacokinetic study of Nom and Atv in mouse plasma in group III, group IV and group V. The plasma concentration-time curves of Nom and Atv in mice plasma were shown in Fig. 3.

The main pharmacokinetic parameters of Nom and Atv were calculated according to the non-compartmental model (Table 1 and Table 2). The $AUC_{0\text{-}t}$ of Nom after intragastric administration in single group and combined group were 344.73 ± 73.70 ng/mL × h and 365.90 ± 89.10 ng/mL × h, with the $T_{1/2}$ of Nom was 2.94 ± 0.06 and 2.91 ± 0.05, respectively. There was no significant difference in the pharmacokinetic parameters of Nom, indicating that the pharmacokinetic behavior of Nom was not affected by Atv. On the other hand, oral administration of Nom (50 mg/kg) could affect the exposure level of Atv *in vivo*. A significantly differed between mice in single group and combined group, with $AUC_{0\text{-}t}$ (69.30 ± 15.45 ng/mL × h) in single group was greater than $AUC_{0\text{-}t}$ (42.37 ± 10.15 ng/mL × h) in combined group ($p < 0.05$). When mice were taken orally 1.67 mg/kg Atv and 1.67 mg/kg Atv & 50 mg/kg Nom, the mean

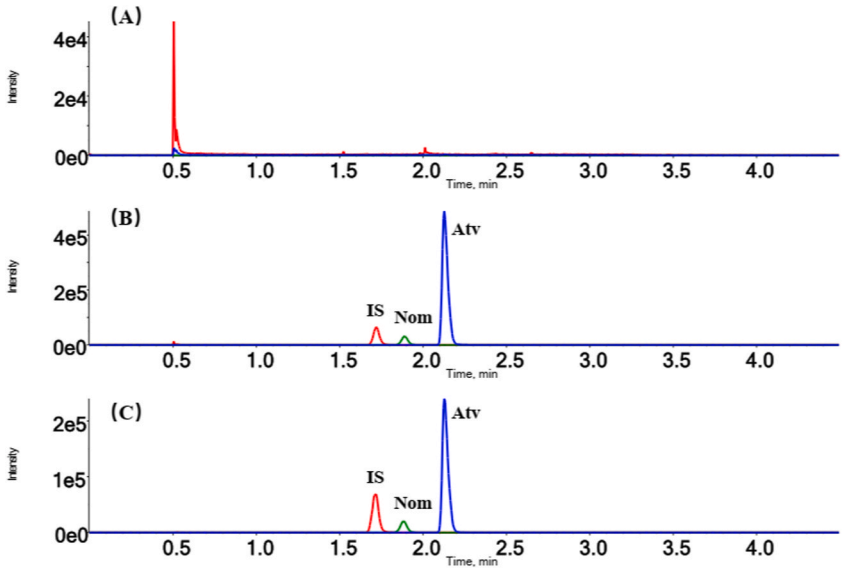

Fig. 2. Representative multiple reaction monitoring (MRM) chromatograms of Nom, Atv and IS in mice plasma: (A) a blank plasma sample; (B) a blank plasma sample spiked with Nom, Atv and IS standards; C, plasma sample collected at 0.5 h after oral administration of Nom and Atv.

C_{max} of Atv reached 18.53 ng/mL and 11.80 ng/mL at 0.50 h in two groups, indicating that Atv could be absorbed into the blood circulation system rapidly. The $T_{1/2}$ and calculated clearance rate (CL/F) were 8.73 ± 0.56 h and 14.94 ± 3.45 L/h/kg in single group and 3.02 ± 0.24 h and 24.58 ± 6.12 L/h/kg in combined group, which showed that Atv had a shorter residence time in circulation and rapid metabolic elimination after co-administration with Nom compared to oral administration alone. Considering that the bioavailability of Atv and Nom was 3.2 % and 4.2 % in mice by other researchers [25,26], the amounts of drug absorbed into the blood were less. Therefore, the calculated Vd/F by oral dosage was relatively large. The calculated Vd/F of Nom (633.98 ± 124.67 and 597.90 ± 154.29 L/kg) were greater than that of Atv (186.45 ± 32.09 and 108.51 ± 35.58 L/kg), indicating that the Nom was probably more widely distributed in the body and has a higher degree of binding with organs than Atv. These results suggested that the absorption and metabolism of Atv may be influenced by metabolic enzymes, transport protein, or related intestinal flora in the gastrointestinal tract through co-administration with Nom.

3.3. Estimation of the serum lipid levels for pharmacodynamic study

The effects of the treatment groups recorded of the study were summarized in Fig. 4. The results of the study were analyzed using one-way ANOVA followed by Dunnett multiple comparison tests. The total lipid profiles of the groups II (model group) were compared with that of the group I (control group) ($p < 0.001, p < 0.01$), indicated that the establishment of hyperlipidemia model was successful. The group III diseased animals treated with Nom alone shows significance decrease in triglycerides (TG) levels ($p < 0.05$) as compared that of group II diseased animals treated with blank 0.5%CMC solution, indicated that Nom could be used for reducing the TG levels. The group IV diseased animals treated with Atv alone shows significance decrease in cholesterol (TC) levels ($p < 0.05$), triglycerides (TG) levels ($p < 0.01$) and LDL cholesterol levels ($p < 0.05$) as compared to that of the diseased group II animals. The results show that as the first line of hypolipidemic drugs, Atv could reduce the important lipid levels of hyperlipidemic mice obviously.

The degree of reduction in lipid levels of the group V diseased animals treated with co-administration of Atv and Nom was less than that of group IV diseased animals treated with Atv alone. The TC and LDL cholesterol levels of mice in combined group (5.75 ± 0.47 mmol/L and 0.75 ± 0.08 mmol/L) show significant difference compared to that of the mice treated with Atv alone (4.94 ± 0.34 mmol/L and 0.55 ± 0.09 mmol/L) ($p < 0.05$). Considering that Atv is an excellent antilipidemic drug, and that orally co-administered Nom significantly reduce the *in vivo* lipid-lowering action of Atv, we speculate that Nom might have contributed to the low oral bioavailability of Atv due to the antagonistic effect.

3.4. Histopathology assessment

The histological changes in the mice liver of all groups were obtained by HE staining in Fig. 5. In the control group, it shown that the structures of liver cells were intact, with clear boundaries, and no obvious pathological abnormalities. In the model group, a large

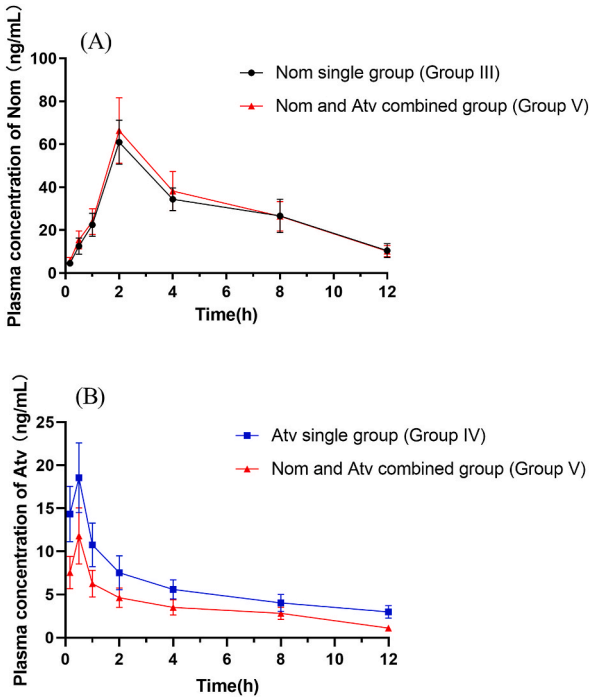

Fig. 3. The mean plasma concentration-time curves of Nom(A) and Atv(B) after the last intragastric administration of Nom (50mg/kg), Atv (1.67 mg/kg) and co-administration with Nom (50 mg/kg) and Atv (1.67 mg/kg) (n = 8).

Table 1
The pharmacokinetic parameters of Nom after intragastric administration of Nom (50 mg/kg) and co-administration with Nom (50 mg/kg) and Atv (1.67 mg/kg) (mean ± SD, n = 8).

Parameters of Nom	Single group	Combined group
AUC_{0-t}(ng/mL × h)	344.73 ± 73.70	365.90 ± 89.10
$AUC_{0-\infty}$(ng/mL × h)	389.20 ± 88.20	408.50 ± 99.45
MRT_{0-t}(h)	6.23 ± 0.31	6.00 ± 0.55
$T_{1/2}$(h)	2.94 ± 0.06	2.91 ± 0.05
T_{max}(h)	2.00 ± 0.00	2.0 ± 0.00
C_{max}(ng/mL)	60.90 ± 10.20	66.30 ± 15.30
Vd/F(L/kg)	633.98 ± 124.67	597.90 ± 154.29
CL/F(L/h/kg)	149.68 ± 32.79	142.41 ± 35.78

Table 2
The pharmacokinetic parameters of Atv after intragastric administration of Atv (1.67 mg/kg) and co-administration with Nom (50 mg/kg) and Atv (1.67 mg/kg) (mean ± SD, n = 8).

Parameters of Atv	Single group	Combined group
AUC_{0-t}(ng/mL × h)	69.30 ± 15.45	42.37 ± 10.15*
$AUC_{0-\infty}$(ng/mL × h)	106.47 ± 26.08	47.10 ± 10.65*
MRT_{0-t}(h)	11.37 ± 0.67	7.43 ± 3.18
$T_{1/2}$(h)	8.73 ± 0.56	3.02 ± 0.24***
T_{max}(h)	0.50 ± 0.00	0.50 ± 0.00
C_{max}(ng/mL)	18.53 ± 4.00	11.80 ± 3.20
Vd/F(L/kg)	186.45 ± 32.09	108.51 ± 35.58*
CL/F(L/h/kg)	14.94 ± 3.45	24.58 ± 6.12

Note: *$p < 0.05$, ***$p < 0.001$, vs pharmacokinetic parameters of Atv of single group and combined group.

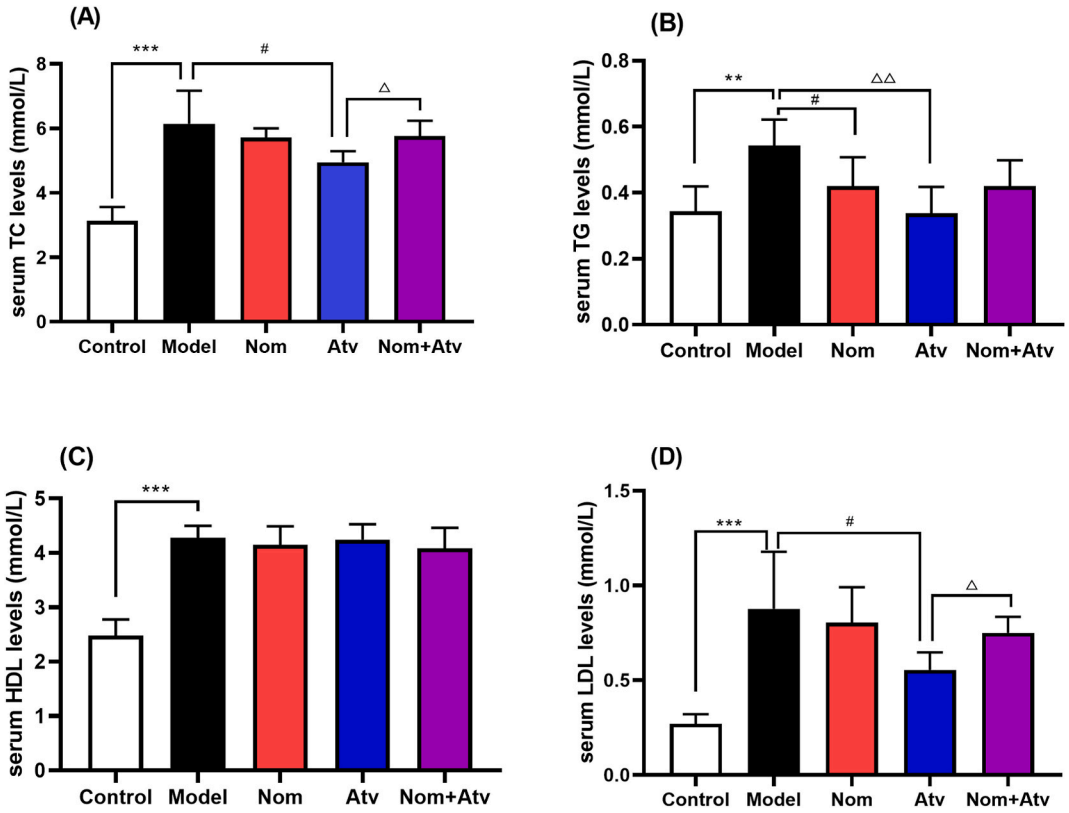

Fig. 4. The lipid levels of hyperlipidemic mice: (A) total cholesterol (TC); (B) triglycerides (TG); (C) high density lipoproteins-cholesterol (HDL-C); (D) low density lipoproteins-cholesterol (LDL-C) (n = 8). Data are expressed as mean ± SD. **$p < 0.01$, ***$p < 0.001$; $^{\#}p < 0.05$, $^{\triangle}p < 0.05$, $^{\triangle\triangle}p < 0.01$ compared with the different groups.

number of liver cells were deformed, dissolved, and formed obvious vacuoles. Amounts of lipid droplet were accumulated in mice livers of the model group. The rest of the mice in the drug administration groups showed different degrees of recovery compared to the model group. In the group of Atv individually administered, no obvious damage and necrosis has been observed. The recovery condition of liver cells in Atv individually administered group was significantly better than Nom individually administered group and the co-administration group of Nom with Atv.

3.5. Determination of hepatic microsomal CYP450 enzyme activities

Three CYP activities were determined in hepatic microsomes using phenacetin for CYP1A2, chlorzoxazone for CYP2E1 and testosterone for CYP3A11, as recommended by the US Food and Drug Administration (2006) for each CYP enzyme were incubated in cocktail assay. The representative MRM typical chromatograms of all metabolites in cocktail assay were shown in Fig. S1. The generated amounts of probe product were used to reflect the enzyme informations in different groups. The hepatic microsomal enzyme levels in Group I – V were shown in Fig. 6.

Compared with the normal mice, the hepatic microsomal CYP1A2, CYP2E1 and CYP3A11 activities were unchanged significantly by high-fat diet treatment. The activities of CYP1A2, CYP2E1 and CYP3A11 were increased in hyperlipidemic mice treated with Nom in group III and group V, especially, the activity of CYP3A11 was significantly increased; whereas, Atv had no effect on the activities of the three CYP enzymes in group IV compared with model group and control group. Large variations in the CYP3A11 activity between different groups were seen. The CYP3A11 activities of diseased animals treated with Nom alone and co-administration of Nom and Atv were 2.34-fold and 2.23-fold higher than that of model group, respectively. The results suggested that the Nom (50 mg/kg) can significantly induce and enhance the activity of CYP3A11 in hyperlipidemic mice. The increase of CYP3A11 enzyme activity led to the decrease of Atv content *in vivo*, which led to the weakening of lipid-lowering effect. The results also confirmed the above-mentioned pharmacodynamic tests.

3.6. Determination of the mRNA levels and protein expressions of CYP3A11

The data in Fig. 7A showed that compared with the control group and model group, the relative mRNA expression levels of CYP3A11 was significantly increased in Nom group and co-administration with Nom and Atv group ($p < 0.001$), while no significant changed was observed in Atv group. The results indicated that Nom (50 kg/mg) induced the elevated relative mRNA expression levels of CYP3A11 in livers of hyperlipidemic mice.

To investigate whether the increase in enzyme gene levels was influenced to the protein expression, the protein expression of CYP3A11 in livers were detected via Western blot. As displayed in Fig. 7B and C, compared with the model group, the protein expression of CYP3A11 was significantly increased in Nom group ($p < 0.05$) and co-administration with Nom and Atv group ($p < 0.01$), but this increase was non-significant in hyperlipidemic mice treated with Atv alone, which was consistent with the mRNA levels (Fig. 7A). Overall, these results confirmed that Nom could up-regulate the gene and protein levels of CYP3A11 at the same time.

In the enzyme activities by cocktailing assay, we found that the addition of Nom significantly increased the activity level of CYP3A11. To further explore the relationship between enzyme activities, gene levels and protein expressions, CYP3A11 in mice livers was evaluated comprehensively. There was study reported that the mice received an intraperitoneal injection of 3-methylcholanthrene (MC, 80 mg/kg), and MC could significantly inhibit the protein and enzyme activity expression of CYP3A11 at 72 h after dosing [27]. In another study, CYP3A11 activity was significantly inhibited by Schisandrol B (SolB) in a dose-dependent manner. However, SolB can significantly induce the protein expression of CYP3A11 to 2.5-fold compared with the vehicle group [28]. Thus it can be seen that protein expressions may differ from the trend of enzyme activity. In our study, Nom exposure *in vivo* resulted in enhance of hepatic CYP3A11 activities, gene levels and protein expressions. Importantly, Nom could induce rather than inhibit CYP3A11, which contrasted with a suppression response seen of most natural products in livers, likely related to altered basal enzymatic transcription, protein and activity levels coherently.

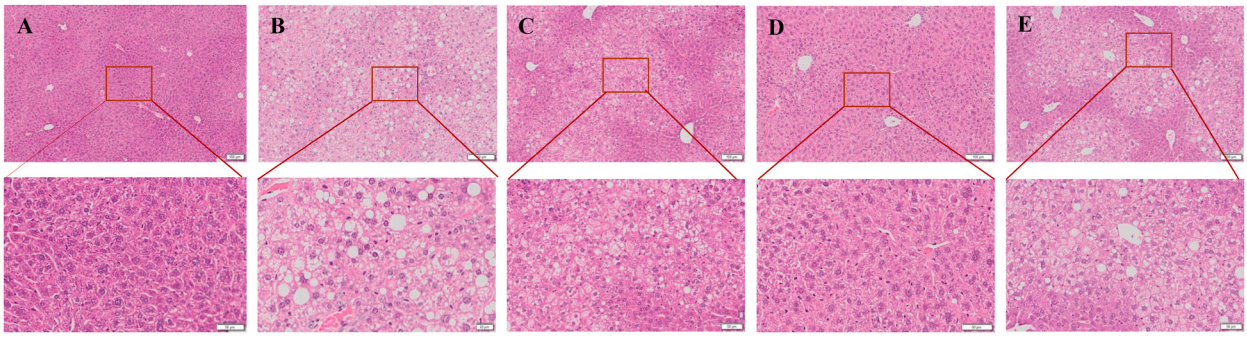

Fig. 5. The HE staining on liver injury. (A) Control group; (B) model group; (C) high fat diet with Nom; (D) high fat diet with Atv; (E) high fat diet with Nom and Atv. (scale bar: 100 μm and 50 μm).

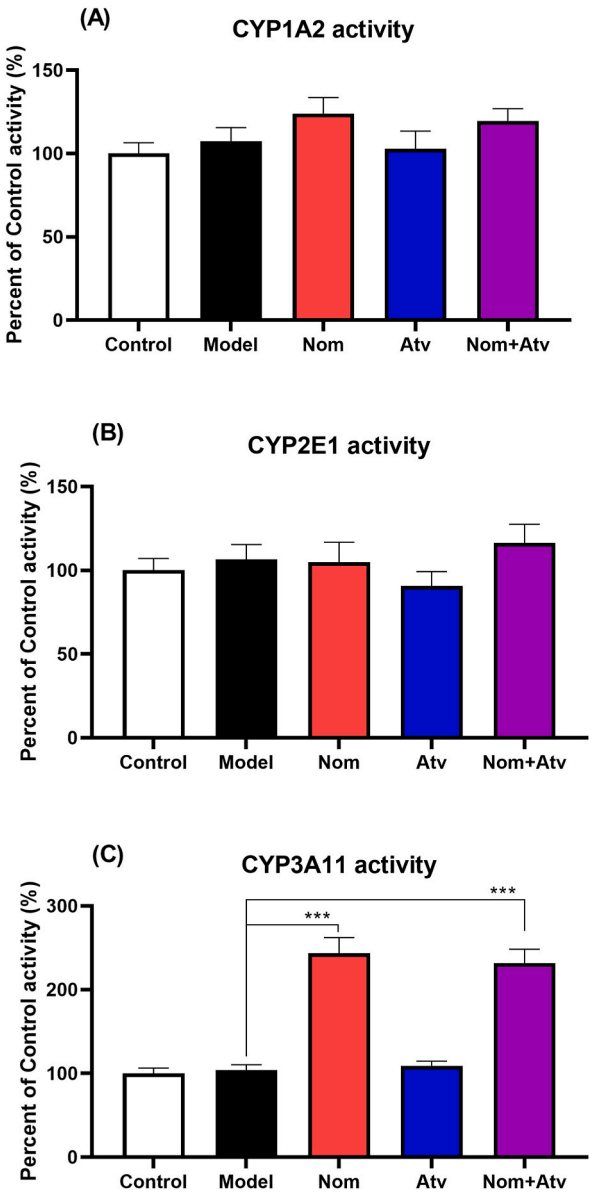

Fig. 6. The hepatic microsomal enzyme activities levels of the hyperlipidemic mice: (A) CYP1A2; (B) CYP2E1 and (C) CYP3A11 (n = 8). Data are expressed as mean ± SD. ***$p < 0.001$ contrasted to the model group.

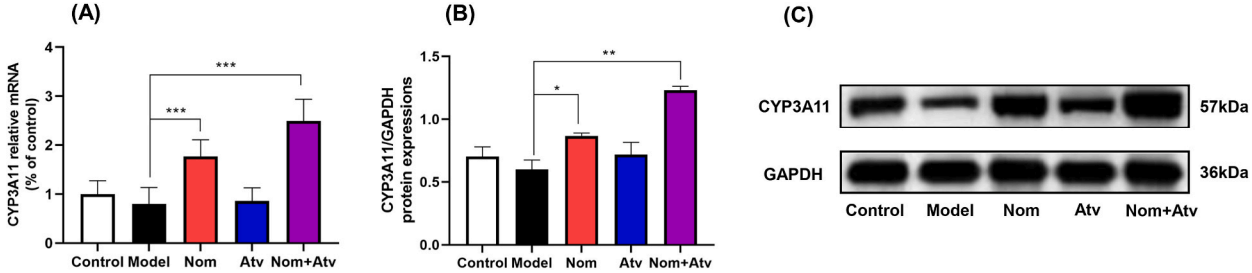

Fig. 7. The relative mRNA expression of CYP3A11 (A) (n = 3) and the protein expression levels of CYP 3A11 (B, C) (n = 3). Data are expressed as mean ± SD. *$p < 0.05$, **$p < 0.01$, ***$p < 0.001$ contrasted to the model group.

4. Conclusion

As the pharmacokinetic profile of Atv was significantly altered on co-administration with Nom, patients with hyperlipidemia treated with Atv and common edible citrus fruits or Chinese medicine preparations containing high content Nom need to requires more emphasis on monitoring. This combination could decrease in bioavailability of Atv, and a decrease in drug concentration of Atv in circulating body fluid may lead to a decrease in the efficacy of lowering hyperlipidemia. This might be related to the effect of Nom on the metabolic enzyme activity, gene and protein levels of CYP3A11 isoenzyme. Hence, the co-administration of Atv and Chinese medicine preparations containing Nom should be taken seriously in clinical use.

CRediT authorship contribution statement

Yan Ding: Funding acquisition, Investigation, Methodology, Project administration, Writing – original draft, Writing – review & editing. **Huida Guan:** Investigation, Methodology, Writing – original draft, Writing – review & editing. **Yingxuan Yan:** Methodology, Validation. **Yan Chen:** Investigation, Validation. **Cheng Huang:** Supervision, Writing – review & editing.

Declaration of competing interest

The authors declare that they have no known competing financialinterestsor personal relationships that could have appeared to influence the work reported in this paper.

Acknowledgements

This work was financially supported by the Science and Technology Development Project of Shanghai University of Traditional Chinese Medicine, China (Grant No. 23KFL021).

Appendix A. Supplementary data

Supplementary data to this article can be found online at https://doi.org/10.1016/j.heliyon.2023.e22016.

References

[1] S. Karr, Epidemiology and management of hyperlipidemia, Am. J. Manag. Care 23 (9 Suppl) (2017) S139–S148.
[2] J. Stewart, T. McCallin, J. Martinez, S. Chacko, S. Yusuf, Hyperlipidemia, Pediatr. Rev. 41 (8) (2020) 393–402. https://doi:10.1542/pir.2019-0053.
[3] R. Balasubramanian, N.M.P. Maideen, HMG-CoA reductase inhibitors (Statins) and their drug interactions involving CYP enzymes, P-glycoprotein and OATP transporters-An overview, Curr. Drug Metabol. 22 (5) (2021) 328–341. https://doi:10.2174/1389200222666210114122729.
[4] S. Li, Y. Yu, Z. Jin, Y. Dai, H. Lin, Z. Jiao, G. Ma, W. Cai, B. Han, X. Xiang, Prediction of pharmacokinetic drug-drug interactions causing atorvastatin-induced rhabdomyolysis using physiologically based pharmacokinetic modelling, Biomed. Pharmacother. 119 (2019), 109416. https://doi:10.1016/j.biopha.2019.109416.
[5] J. Shin, D.F. Pauly, M.A. Pacanowski, T. Langaee, R.F. Frye, J.A. Johnson, Effect of cytochrome P450 3A5 genotype on atorvastatin pharmacokinetics and its interaction with clarithromycin, Pharmacotherapy 31 (10) (2011) 942–950. https://doi:10.1592/phco.31.10.942.
[6] G.S. Clemente, I.F. Antunes, J.W.A. Sijbesma, A. van Waarde, A.A. Lammertsma, A. Dömling, P.H. Elsinga, [^{18}F]Atorvastatin pharmacokinetics and biodistribution in healthy female and male rats, Mol. Pharm. 18 (9) (2021) 3378–3386. https://doi:10.1021/acs.molpharmaceut.1c00305.
[7] O. Croitoru, A.M. Spiridon, I. Belu, A. Turcu-Ştiolică, J. Neamţu, Development and validation of an HPLC method for simultaneous quantification of clopidogrel bisulfate, its carboxylic acid metabolite, and atorvastatin in human plasma: application to a pharmacokinetic study, J Anal Methods Chem 2015 (2015), 892470. https://doi:10.1155/2015/892470.
[8] A.B. Thomas, D.C. Choudhary, A. Raje, S.S. Nagrik, Pharmacokinetics and pharmacodynamic herb-drug interaction of piperine with atorvastatin in rats, J. Chromatogr. Sci. 59 (4) (2021) 371–380. https://doi:10.1093/chromsci/bmaa126.
[9] G.R. Wilkinson, Drug metabolism and variability among patients in drug response, N. Engl. J. Med. 352 (21) (2005) 2211–2221. https://doi:10.1056/NEJMra032424.
[10] H. Lennernäs, Clinical pharmacokinetics of atorvastatin, Clin. Pharmacokinet. 42 (13) (2003) 1141–1160. https://doi:10.2165/00003088-200342130-00005.
[11] Y.Y. Lau, Y. Huang, L. Frassetto, L.Z. Benet, Effect of OATP1B transporter inhibition on the pharmacokinetics of atorvastatin in healthy volunteers, Clin. Pharmacol. Ther. 81 (2) (2007) 194–204. https://doi:10.1038/sj.clpt.6100038.
[12] G.D. Manners, Citrus limonoids: analysis, bioactivity, and biomedical prospects, J. Agric. Food Chem. 55 (21) (2007) 8285–8294. https://doi:10.1021/jf071797h.
[13] Y. Kimira, Y. Taniuchi, S. Nakatani, Y. Sekiguchi, H.J. Kim, J. Shimizu, M. Ebata, M. Wada, A. Matsumoto, H. Mano, Citrus limonoid nomilin inhibits osteoclastogenesis in vitro by suppression of NFATc1 and MAPK signaling pathways, Phytomedicine 22 (12) (2015) 1120–1124. https://doi:10.1016/j.phymed.2015.08.013.
[14] S. Mouly, C. Lloret-Linares, P.O. Sellier, D. Sene, J.F. Bergmann, Is the clinical relevance of drug-food and drug-herb interactions limited to grapefruit juice and Saint-John's Wort? Pharmacol. Res. 118 (2017) 82–92. https://doi:10.1016/j.phrs.2016.09.038.
[15] X.H. Xue, J.X. Xue, W. Hu, F.L. Shi, Y. Yang, Nomilin targets the Keap1-Nrf2 signalling and ameliorates the development of osteoarthritis, J. Cell Mol. Med. 24 (15) (2020) 8579–8588. https://doi:10.1111/jcmm.15484.
[16] M. Minamisawa, S. Yoshida, A. Uzawa, The functional evaluation of waste yuzu (Citrus junos) seeds, Food Funct. 5 (2) (2014) 330–336. https://doi:10.1039/c3fo60440c.
[17] Y.S. Shi, Y. Zhang, B. Liu, C.B. Li, J. Wu, Y. Li, Nomilin protects against cerebral ischemia-reperfusion induced neurological deficits and blood-brain barrier disruption via the Nrf2 pathway, Food Funct. 10 (9) (2019) 5323–5332. https://doi:10.1039/c9fo01481k.
[18] R. Sato, Nomilin as an anti-obesity and anti-hyperglycemic agent, Vitam. Horm. 91 (2013) 425–439. https://doi:10.1016/B978-0-12-407766-9.00018-3.

[19] L. Shi, Z. Jiang, B. Zhang, C. Tang, R.A. Xu, Development of UPLC-MS/MS method for studying the pharmacokinetic interactions of pexidartinib with antifungal drugs in rats, J. Pharm. Biomed. Anal. 188 (2020), 113386. https://doi:10.1016/j.jpba.2020.113386.
[20] S. Xie, L. Ye, X. Ye, G. Lin, R.A. Xu, Inhibitory effects of voriconazole, itraconazole and fluconazole on the pharmacokinetic profiles of ivosidenib in rats by UHPLC-MS/MS, J. Pharm. Biomed. Anal. 187 (2020), 113353. https://doi:10.1016/j.jpba.2020.113353.
[21] W. Li, S. Wang, W. Wang, L. Gong, D. Ni, Y. Li, W. Wu, Y. Zhang, X. Xu, Q. Jiang, J. Zhang, T. Zhang, Ultra-high performance supercritical fluid chromatography-tandem mass spectrometry method for simultaneous determination of atorvastatin, 2-hydroxy atorvastatin, and tangeretin in rat plasma and its application to the pharmacokinetic study, J. Separ. Sci. 45 (21) (2022) 3985–3994. https://doi:10.1002/jssc.202200185.
[22] F.D. Administration, USFDA, Guidance for Industry: Bioanalytical Method Validation, vol. 66, 2001. http://www.fda.gov./cder/guidance/4252fnl.pdf.
[23] L.Y. Liu, Y.L. Han, J.H. Zhu, Q. Yu, Q.J. Yang, J. Lu, C. Guo, A sensitive and high-throughput LC-MS/MS method for inhibition assay of seven major cytochrome P450s in human liver microsomes using an in vitro cocktail of probe substrates, Biomed. Chromatogr. 29 (3) (2015) 437–444. https://doi:10.1002/bmc.3294.
[24] Y. Jiang, X. Fan, Y. Wang, H. Tan, P. Chen, H. Zeng, M. Huang, H. Bi, Hepato-protective effects of six schisandra lignans on acetaminophen-induced liver injury are partially associated with the inhibition of CYP-mediated bioactivation, Chem. Biol. Interact. 231 (2015) 83–89. https://doi:10.1016/j.cbi.2015.02.022.
[25] J.W. Higgins, J.Q. Bao, A.B. Ke, J.R. Manro, J.K. Fallon, P.C. Smith, M.J. Zamek-Gliszczynski, Utility of Oatp1a/1b-knockout and OATP1B1/3-humanized mice in the study of OATP-mediated pharmacokinetics and tissue distribution: case studies with pravastatin, atorvastatin, simvastatin, and carboxydichlorofluorescein, Drug Metab. Dispos. 42 (1) (2014) 182–192. https://doi:10.1124/dmd.113.054783.
[26] Y. Cai, S. Zhang, Q. Wang, H. Sun, M. Zhou, S. Hu, Z. Xiang, A rapid, selective and sensitive UPLC-MS/MS method for quantification of nomilin in rat plasma and its application in a pharmacokinetic study, Planta Med. 82 (3) (2016) 224–229. https://doi:10.1055/s-0035-1558157.
[27] M. Crosby, D.S. Riddick, Suppression of hepatic CYP3A4 expression and activity by 3-methylcholanthrene in humanized PXR-CAR-CYP3A4/3A7 mice, Drug Metab. Dispos. 47 (3) (2019) 279–282. https://doi:10.1124/dmd.118.084509.
[28] Y. Jiang, X. Fan, Y. Wang, P. Chen, H. Zeng, H. Tan, F.J. Gonzalez, M. Huang, H. Bi, Schisandrol B protects against acetaminophen-induced hepatotoxicity by inhibition of CYP-mediated bioactivation and regulation of liver regeneration, Toxicol. Sci. 143 (1) (2015) 107–115. https://doi:10.1093/toxsci/kfu216.